

Modern Physics Letters A
 © World Scientific Publishing Company

High-spin structures of $^{77,79,81,83}\text{As}$ isotopes

VIKAS KUMAR, P.C. SRIVASTAVA*

Department of Physics, Indian Institute of Technology, Roorkee - 247 667, India

IRVING O. MORALES

Instituto de Ciencias Nucleares, Universidad Nacional Autónoma de México, 04510 México, D.F., Mexico

In the present work we report comprehensive set of shell model calculations for arsenic isotopes. We performed shell model calculations with two recent effective interactions JUN45 and jj44b. The overall results for the energy levels and magnetic moments are in rather good agreement with the available experimental data. We have also reported competition of proton- and neutron-pair breakings analysis to identify which nucleon pairs are broken to obtain the total angular momentum of the calculated states. Further theoretical development is needed by enlarging model space by including $\pi 0f_{7/2}$ and $\nu 1d_{5/2}$ orbitals.

Keywords: Model space; effective interaction.

21.60.Cs, 27.50.+e

1. Introduction

The neutron rich nuclei of the Segré chart near Ni region has contributed valuable input for the understanding of nuclear shell evolution.^{1,2,3,4,5,6,7,8} It is demonstrated that the shell evolution in nuclei mainly have two types, first type one in which evolution of nuclear shell as a function of N or Z and second type evolution normally occur within the same nucleus.⁹ Recently experimental evidence for the doubly magic ($Z = 20$ and $N = 34$) nature of ^{54}Ca with the onset of a sizable subshell closure at $N = 34$ is reported in Ref.¹

In the case of Cu isotopes it has been shown that around $N = 40$ the proton single-particle ordering changes when neutrons start occupying $g_{9/2}$ orbital.¹⁰ The systematics of the $1/2^-$, $3/2^-$ and $5/2^-$ levels, magnetic and electric quadrupole moments between $N = 40$ to $N = 50$ for Ga isotopes is reported in Ref.¹¹ For ^{79}Ga the $\pi f_{5/2}$ orbital dominant in the g.s. While, for ^{81}Ga , $5/2^-$ level become ground state. This is due to emptying of $\pi p_{3/2}$ orbital to $\pi f_{5/2}$ is started as we move from ^{71}Ga to ^{79}Ga . Ultimately, $1^{\pi}=5/2^-$ become ground state for ^{81}Ga . The systematics of low-lying yrast states in case of As isotopes is shown in Fig. 1. In case

*Email: pcsrifph@iitr.ac.in

2 *Kumar, Srivastava, and Morales*

of $^{73-81}\text{As}$, the g.s. is $3/2^-$, while for ^{83}As again $5/2^-$ become g.s. In the recent work, Porquet et al.¹² suggested that $f_{5/2}pg_{9/2}$ space is not enough to explain quadrupole excitation built on the $5/2_1^-$ and $9/2_1^+$ state of ^{81}As . Theoretical results for $^{67-79}\text{As}$ isotopes with projected shell model recently reported in Ref.¹³

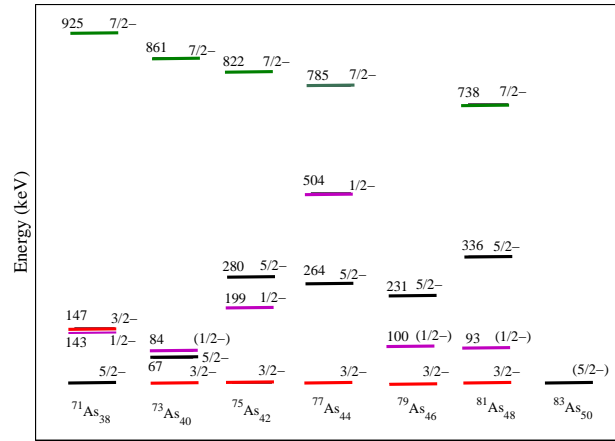


Fig. 1. Low lying yrast states in ^{71}As to ^{83}As covering $N=40$ to $N=50$ shell closure.

2. Outline of Calculations

In the present work we have performed calculations in the $f_{5/2}pg_{9/2}$ space. We have performed calculations with recently available effective interactions JUN45¹⁴ and jj44b.¹⁵ In case of JUN45, the single-particle energies for the $1p_{3/2}$, $0f_{5/2}$, $1p_{1/2}$ and $0g_{9/2}$ orbits are -9.8280, -8.7087, -7.8388, and -6.2617 MeV respectively. For jj44b interaction they are -9.6566, -9.2859, -8.2695, and -5.8944 MeV, respectively. The core is ^{56}Ni , i.e. $N = Z = 28$, and the calculations are performed in this valence space without truncation. The JUN45 interaction is based on Bonn-C potential, the single-particle energies and two-body matrix elements was modified empirically with $A = 63\sim 69$. Similarly the jj44b interaction was obtained from a fit to binding energies and excitation energies with 30 linear combinations of the good $J - T$ two-body matrix elements. The calculations were performed with shell-model codes ANTOINE¹⁶ and NuShellX.¹⁷

3. Spectra analysis

The shell model results for $^{77,79,81,83}\text{As}$ isotopes are presented with respect to the experiment in Figs. 2-5.

3.1. ^{77}As

Comparison of calculated energy levels of ^{77}As with experimental data is shown in Fig. 2. The JUN45 and jj44b interactions predicted $3/2^-$ level as a ground state which is in good agreement with experiment. Level $1/2_1^-$ is the first excited state predicted by JUN45 and jj44b. The calculations predicting $1/2_1^-$ level lower than the experiment. The sequence of the experimentally observed energy levels $3/2_2^-$ and $5/2_1^-$ are same in jj44b while it is interchanged in JUN45. The overall values of energy levels of $3/2_2^-$ and $5/2_1^-$ with jj44b is in good agreement with experiment. The calculated $3/2_2^-$ energy level by two effective interactions are higher than experiment. The JUN45 predict $1/2_2^-$ level at 411 keV, jj44b at 1181 keV, but experiment predicted it at 2195 keV. The levels $9/2_1^-$ and $7/2_2^-$ calculated by both interactions are in good agreement with experiment. While levels $5/2_2^-$ and $13/2_1^-$ predicted by two interactions are lower than the experiment. The $7/2_3^-$ level calculated by JUN45 is in good agreement with experiment while with jj44b it is 303 keV higher than the experiment. The sequence of the calculated high-spin negative parity energy levels by JUN45 and jj44b interactions are in good agreement with experiment. In the case of positive parity, JUN45 and jj44b predict $9/2_1^+$ as a lowest positive parity state and $5/2_1^+$ as a second positive parity state which is in good agreement with experiment but these levels are higher than the experimental values. The level $7/2_1^+$ calculated by JUN45 and jj44b are higher than the experiment and $7/2_2^+$ level is lower with both JUN45 and jj44b. The energy separation between $7/2_1^+$ and $7/2_2^+$ is 197 keV in JUN45, 204 keV in jj44b while in the experiment it is 1194 keV. Experimentally observed two consecutive levels, $5/2_2^+$ and $5/2_3^+$ are higher in both calculations and there are five levels ($7/2_1^+$, $11/2_1^+$, $13/2_1^+$, $7/2_2^+$ and $9/2_2^+$) between them in jj44b. The JUN45 and jj44b interactions predicted $\pi(p_{3/2}^3)$ configuration for g.s. $3/2_1^-$ with probability 15.7% and 13.6%, respectively. The structure of negative parity states from $3/2_1^-$ to $19/2_1^-$ is mainly from $\pi(p_{3/2}f_{5/2})^5$ configuration. In the case of positive parity, the structure for $9/2_1^+$ state is $\pi(g_{9/2}^1)$, with probability 11.4% (JUN45) and 16.9% (jj44b). The occupancy of $\pi g_{9/2}$ orbital for $9/2_1^+$ state is 1.06 (JUN45) and 1.07 (jj44b).

3.2. ^{79}As

In the Fig. 3, we have shown the comparison of the values of the energy levels calculated by JUN45 and jj44b with experimental data for ^{79}As . The JUN45 predict $3/2^-$ level as a ground state which is in good agreement with experiment, where as jj44b predicts $1/2^-$ as a ground state which is different from experiment. The levels $3/2_1^-$ and $1/2_1^-$ are interchanged in jj44b. The levels $3/2_2^-$ and $5/2_1^-$ calculated by jj44b are in good agreement with experiment values. The calculated $3/2_3^-$ level with jj44b is in good agreement with experiment while with JUN45 it is lower by 414 keV than the experiment.

The calculated value of level $5/2_3^-$ with both interactions are lower than the

experiment. The calculated positive parity levels are higher with both interactions than the experiment. For positive parity, the JUN45 and jj44b predicts $9/2^+$ as lowest positive parity state which is also predicted by experiment but it is higher by 656 keV in JUN45 and by 1011 keV in jj44b than the experiment. As in the experiment the next positive parity state is $5/2^+$ by JUN45, while it is at higher energy with jj44b interaction. In the experiment after $9/2_2^+$ next one is $9/2_3^+$ but in between these two levels JUN45 predict two more levels ($5/2_2^+$ at 2345 keV and $5/2_3^+$ at 2374 keV), while in jj44b five levels ($1/2_1^+$ at 2129 keV, $5/2_1^+$ at 2194 keV, $5/2_2^+$ at 2221 keV, $1/2_2^+$ at 2270 keV, $5/2_3^+$ at 2402 keV). In jj44b calculation the $1/2_1^+$ and $1/2_2^+$ levels are lower than $9/2_3^+$ in comparison to the experiment value.

The JUN45 and jj44b interactions predicted $\pi(p_{3/2}^1)$ configuration for g.s. ($3/2_1^-$) with probability 12.7% and 10.1%, respectively. The structure of negative parity states from $3/2_1^-$ to $19/2_1^-$ are mainly from $\pi(p_{3/2}f_{5/2})^5$ configuration. In the case of positive parity, the structure for $9/2_1^+$ state is $\pi(g_{9/2}^1)$, with probability 16.4% (JUN45) and 12.4% (jj44b). The occupancy of $\pi g_{9/2}$ orbital for $9/2_1^+$ state is 1.07 (JUN45) and 1.06 (jj44b).

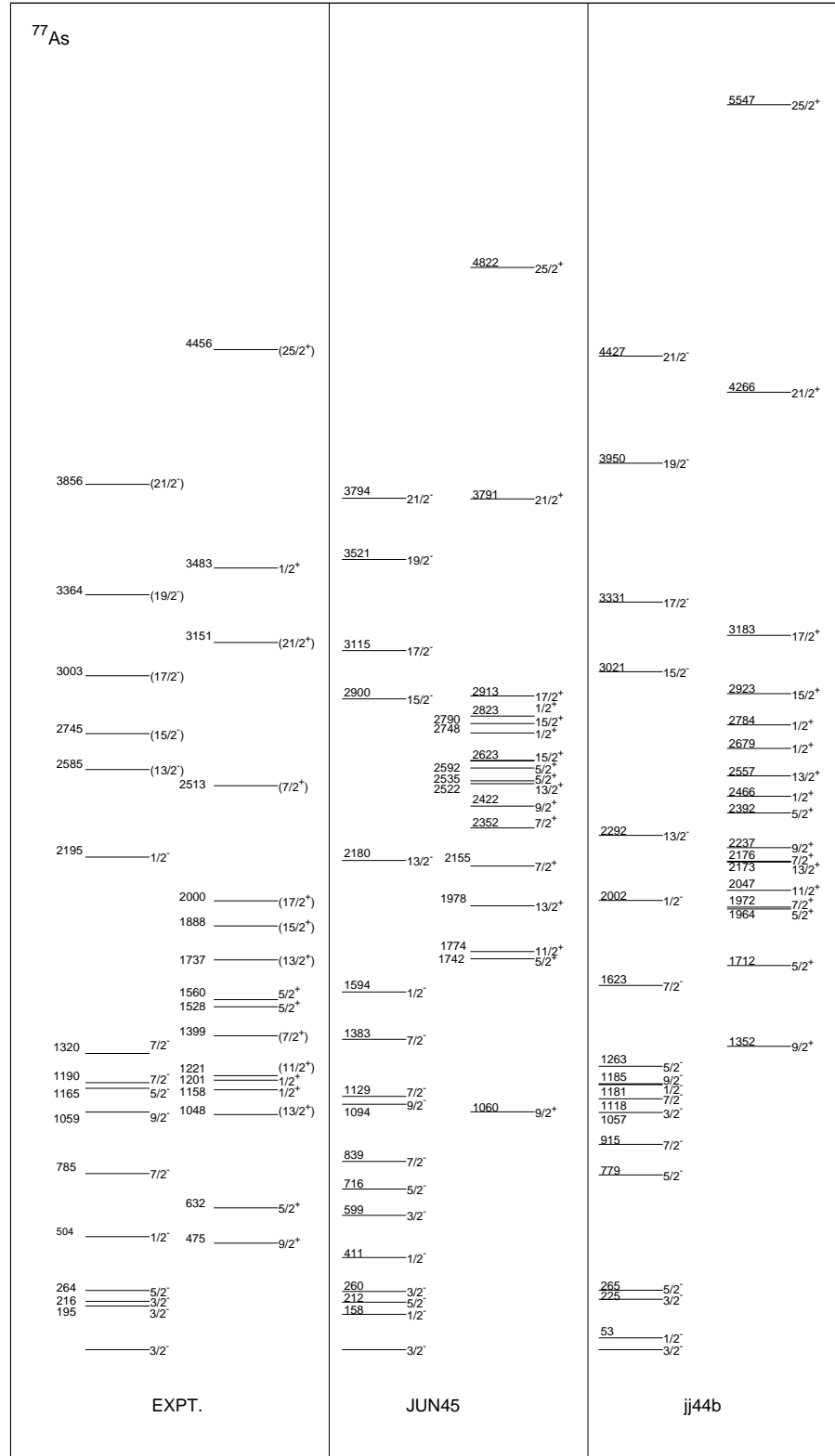
3.3. ^{81}As

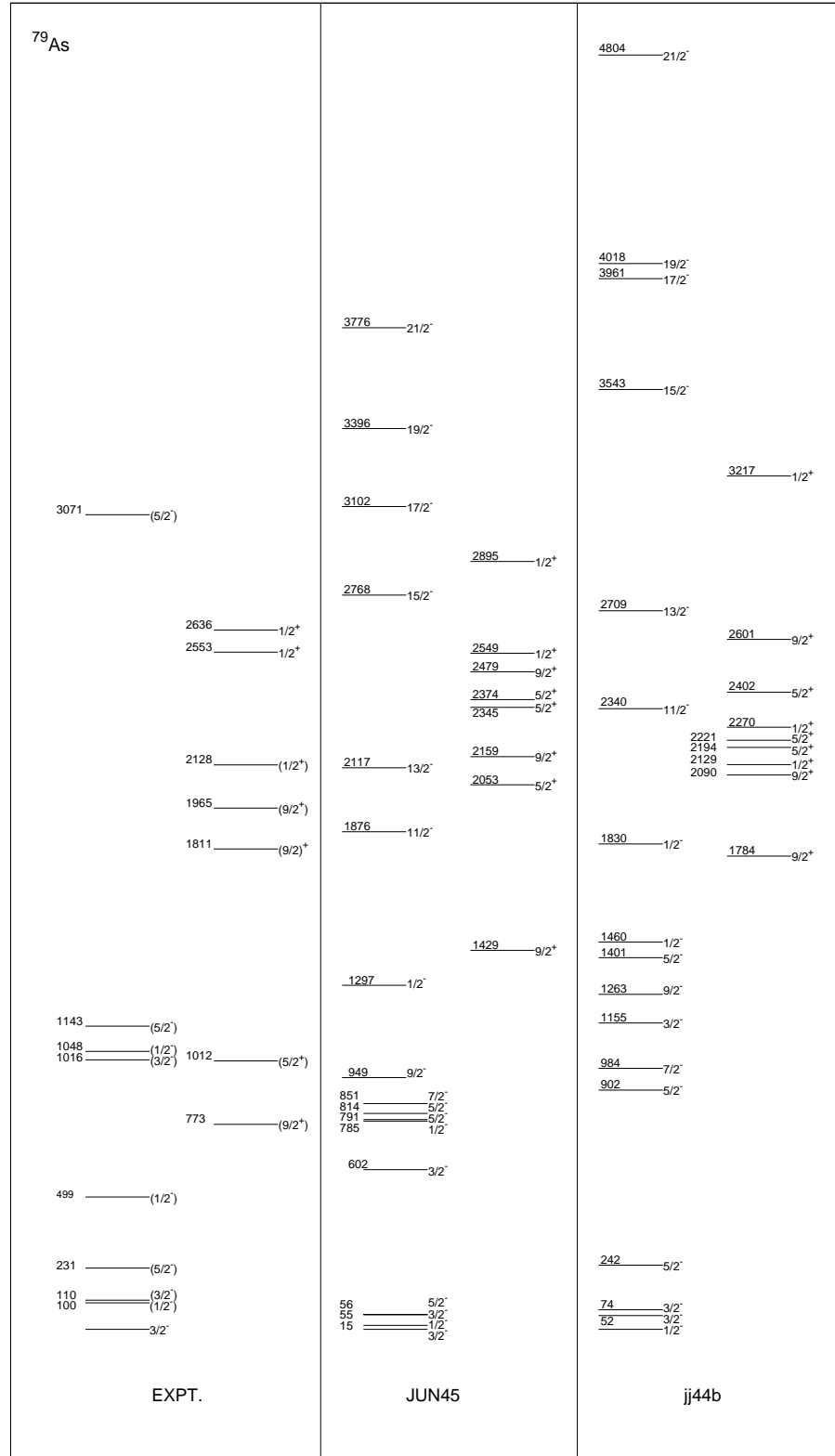
In the Fig. 4, we have shown results for ^{81}As , the calculated $3/2_2^-$ and $5/2_1^-$ levels by jj44b are in good agreement with experiment, while with JUN45 these levels are interchanged. The JUN45 and jj44b predicted higher value of $7/2_1^-$ by 142 keV, 151 keV, respectively, and lower value of $3/2_3^-$ by 2026 keV, 1689 keV respectively than the experiment. The level $7/2_2^-$ predicted by JUN45 is higher by 94 keV, but it is further higher by 279 keV in jj44b. The calculated $9/2_1^-$ and $13/2_1^-$ levels by JUN45 are in good agreement with experiment but it is predicted at higher value by jj44b. The level $17/2_1^-$ calculated by both interactions are in good agreement with experiment. The JUN45 and jj44b predicted $21/2_1^-$ level higher by 734 and 882 keV, respectively than the experimental result.

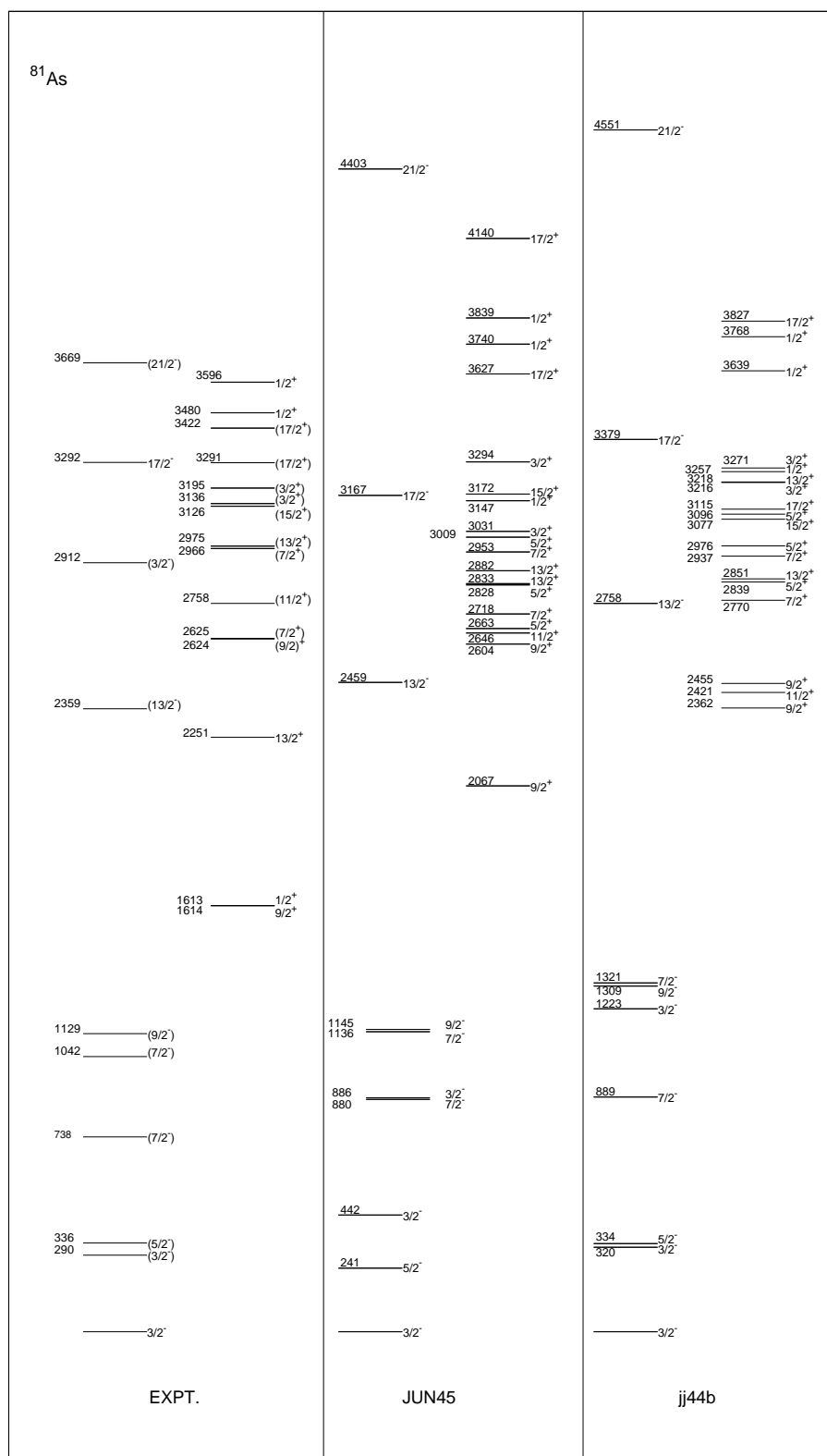
For the positive parity, JUN45 and jj44b predicted $9/2^+$ as a lowest positive parity state as in the experiment but this level is at higher energy than the experimental value. Both the calculations predicting higher value of the level $13/2_1^+$ than the experimental value. As we approach towards $N = 50$, it is now important to include $\nu 1d_{5/2}$ orbital in the model space to study neutron excitation across $N = 50$ shell.

3.4. ^{83}As

We have shown results for ^{83}As in Fig. 5. Both the interactions JUN45 and jj44b predicted g.s. as a $5/2^-$. The levels $9/2_1^-$ and $11/2_1^-$ are lowered by 132 and 141 keV in JUN45 whereas both levels are higher by 165 and 173 keV in jj44b. With JUN45 $13/2_1^-$ level is in good agreement while in jj44b it is higher by 154 keV than the experiment. The sequence of energy levels $5/2_1^-$, $9/2_1^-$, $11/2_1^-$ and $13/2_1^-$ in jj44b are in good agreement with experiment. The JUN45 and jj44b predicts $9/2^+$

High-spin structures of $^{77,79,81,83}\text{As}$ isotopes 5Fig. 2. Comparison of experimental and calculated excitation spectra of ^{77}As .

6 *Kumar, Srivastava, and Morales*Fig. 3. Comparison of experimental and calculated excitation spectra of ⁷⁹As.

High-spin structures of $^{77,79,81,83}\text{As}$ isotopes 7Fig. 4. Comparison of experimental⁶ and calculated excitation spectra of ^{81}As .

as a lowest positive parity state. While there is no experimental result is available for positive parity. All the positive parity states predicted by jj44b is lower than JUN45.

4. Competition of proton- and neutron-pair breakings analysis

In Figs. 6-7 we have shown decomposition of the total angular momentum of the selected states for $^{79,81}\text{As}$ isotopes with JUN45 interaction. From the analysis of the wavefunctions it is possible to identify which nucleon pairs are broken to obtain the total angular momentum of the calculated states. The two components for neutrons and protons are I_n and I_p respectively. These components are coupled to give the total angular momentum of each states. In the Fig. 6(a) -(d), we have shown results of negative parity states of ^{79}As . The dominant component (46 %) of the $3/2_1^-$ ground state comes from $I_p = 3/2$. The $1/2_1^-$ comes from $I_p = 1/2$ (40 %), $5/2_1^-$ comes from $I_p = 5/2$ (47 %), $7/2_1^-$ comes from $I_p = 7/2$ (28 %). The $17/2_1^-$ state has a very peculiar wave function. It shows many different components (35 % of $5/2_p^- \otimes 6_n^+$, 18 % of $9/2_p^- \otimes 4_n^+$, 14 % of $3/2_p^- \otimes 8_n^+$, ...), thus resembling a "collective" state. The wave function of $19/2_1^-$ state (predicted at 3396 keV) have the major one corresponding to $I_p = 3/2 \otimes I_n = 8$ (44 %) and the minor one to $I_p = 7/2 \otimes I_n = 6$ (14 %). Further the wave function of $21/2_1^-$ state (predicted at 3776 keV) have the major one corresponding to $I_p = 5/2 \otimes I_n = 8$ (57 %) and the minor one to $I_p = 9/2 \otimes I_n = 6$ (11 %). In the Fig. 6(e) -(h), we have shown results of positive parity states of ^{79}As . The major component of $9/2_1^+$ comes from $I_p = 9/2$ (40 %). Similarly $5/2_1^+$ comes from $I_p = 5/2$ (30 %).

In the Fig. 7(a) -(d), we have shown results of negative parity states of ^{81}As . The $3/2_1^-$ comes from $I_p = 3/2$ (55 %). The $17/2_1^-$ comes mainly from $I_n = 8$ (with $I_p = 1/2 - 7/2$), i.e. due to neutron pair breaking. Similarly the $21/2_1^-$ (at 4403 keV) from $I_n = 8$ (with $I_p = 5/2 - 9/2$). The $13/2_1^-$ shows many different components (43 % of $9/2_p^- \otimes 2_n^+$, 23 % of $5/2_p^- \otimes 4_n^+$, 16 % of $13/2_p^- \otimes 0_n^+$, ...), thus resembling a "collective" state. The positive parity states results are shown in Fig. 7(e) -(h). The major component of $9/2_1^+$ comes from $I_p = 9/2$ (59 %). The $9/2_2^+$ and $17/2_1^+$ is coming from pure neutron breaking. The $1/2_1^+$ shows many different components (65 % of $5/2_p^+ \otimes 3_n^+$, ...), thus resembling a "collective" state. The above three families are drawn with three different colors, the magenta color is for breaking of neutron pairs, the green color is for that of protons and blue color is for many components with various values of I_n and I_p .

5. Electromagnetic properties and occupation numbers analysis

5.1. $E2$ transition probability, quadrupole and magnetic moments

In Table 1 and 2, we have shown calculated $B(E2)$ and $B(M1)$ values for different transitions. Although experimental data are very sparse. For $B(E2:5/2_1^+ \rightarrow 9/2_1^+)$, the result of jj44b interaction is better than JUN45. It is further improve by increasing effective charges. The experimental $B(M1)$ values are only available for ^{79}As ,

for $\text{BM1}(5/2_1^- \rightarrow 3/2_1^-)$ transition the predicted value of JUN45 interaction is close to experimental value. In Table 3, we have also compared results of quadrupole and magnetic moments.

The overall results of magnetic moments are in good agreement with the available experimental data and also the differences between the results obtained by the two adopted interactions are reasonable. On the other hand it is not possible to draw some definite conclusions for the $B(E2)$ and quadrupole moments due to lack of experimental data and contradictory results for the $B(E2)$ values. The calculated results for $B(E2)$ and quadrupole moments for two interactions are different. This may be because two interactions were obtained from a fit with experimental data of different set of nuclei. The JUN45 interaction derived by fitting 400 experimental binding and excitation energy data out of 69 nuclei in the $A = 63 \sim 96$ mass region while jj44b interaction developed by fitting binding energies and excitation energies from nuclei with $Z = 28 - 30$ and $N = 48 - 50$. The jj44b results are better near $Z = 28$. The JUN45 interaction is successful along the $N \sim 50$ isotone chains, while for the Ni region, the results are not satisfactory, because of the exclusion of the effect of $\pi f_{7/2}$ excitations.¹⁴

5.2. Occupation numbers

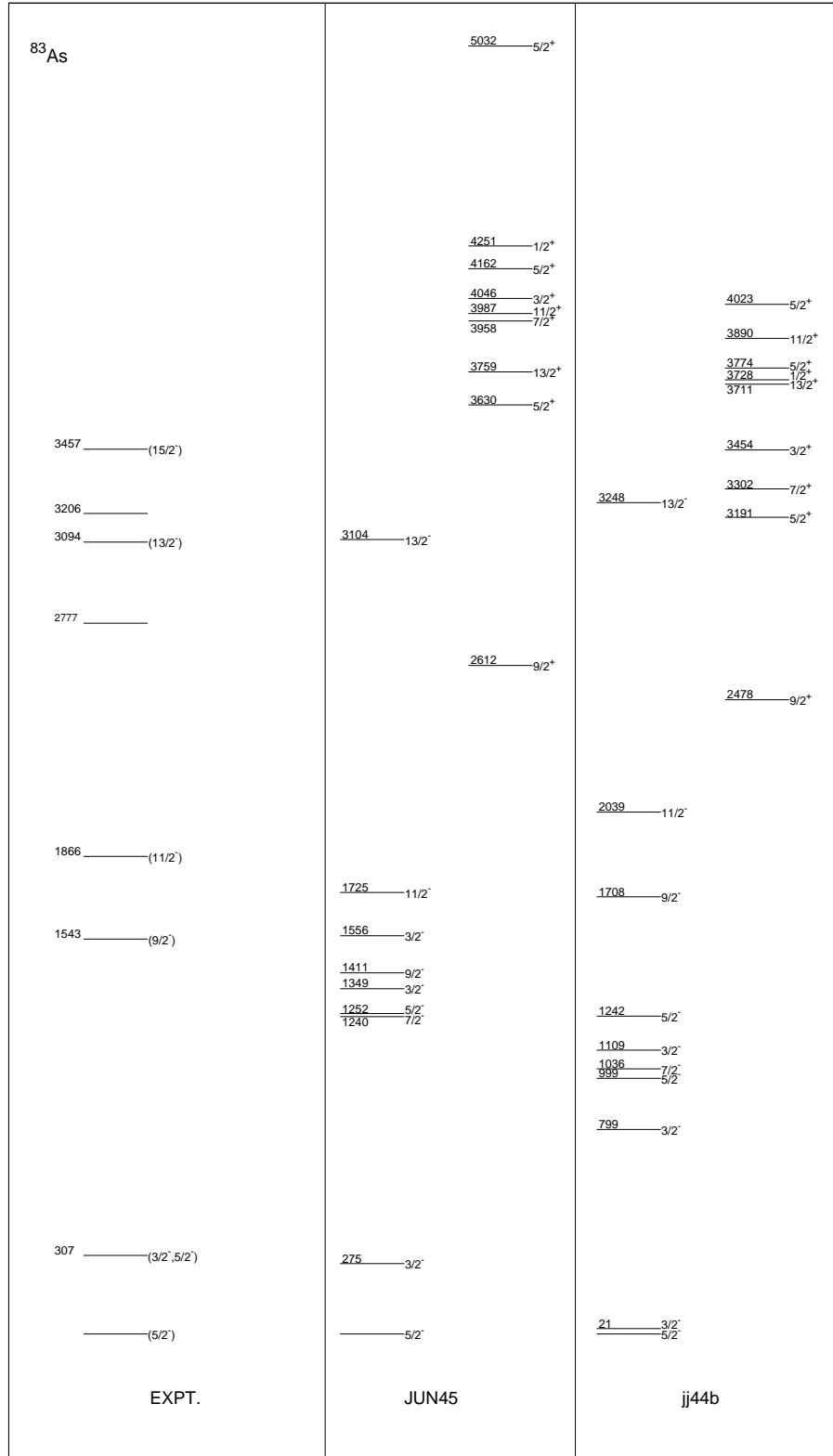
In Fig. 8, we show the proton/neutron occupation numbers. For the ground state ($3/2^-$), the occupancy of $\pi(0f_{5/2})$ orbital increase smoothly, while occupancy of $\pi(1p_{3/2})$ orbital is decreasing. For $9/2^+$, the occupancy of $\pi(0g_{9/2})$ orbital is significant. In the case of neutrons orbital the occupancy of the $\nu(0g_{9/2})$ orbital increases drastically as neutrons number increase from $N = 44$ (^{77}As) to $N = 50$ (^{81}As).

6. Summary

In summary, comprehensive study for the structure of neutron-rich odd-even As isotopes have been carried out using large-scale shell-model calculations for full $f_{5/2}pg_{9/2}$ space with JUN45 and jj44b effective interactions. The overall results for the energy levels and magnetic moments are in good agreement with the available experimental data. The experimental data for $B(E2)$ and quadrupole moments are not available thus it is not possible to draw some definite conclusions. We have also predicted electromagnetic properties for other transitions as a guide for future experimental work.

Further, the following broad conclusions are:

- The results of JUN45 interaction is better than jj44b.
- High-spin states in $^{77,79,81,83}\text{As}$ isotopes comes from breaking of neutron/proton pairs.
- Further theoretical development is needed by enlarging model space by including $\pi 0f_{7/2}$ and $\nu 1d_{5/2}$ orbitals to study simultaneously proton and neutron excitations across $Z = 28$ and $Z = 50$ shell, respectively.

Fig. 5. Comparison of experimental⁶ and calculated excitation spectra of ^{83}As .

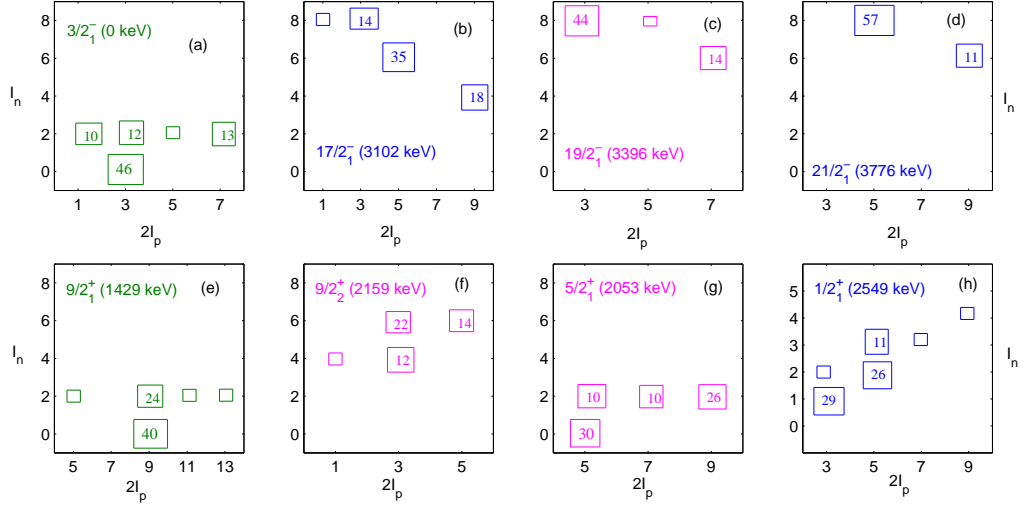


Fig. 6. Decomposition of the total angular momentum of selected states of ^{79}As into their $I_n \otimes I_p$ components. The percentage above 10% are written inside the squares, drawn with an area proportional to it. Percentage below 5% are not written.

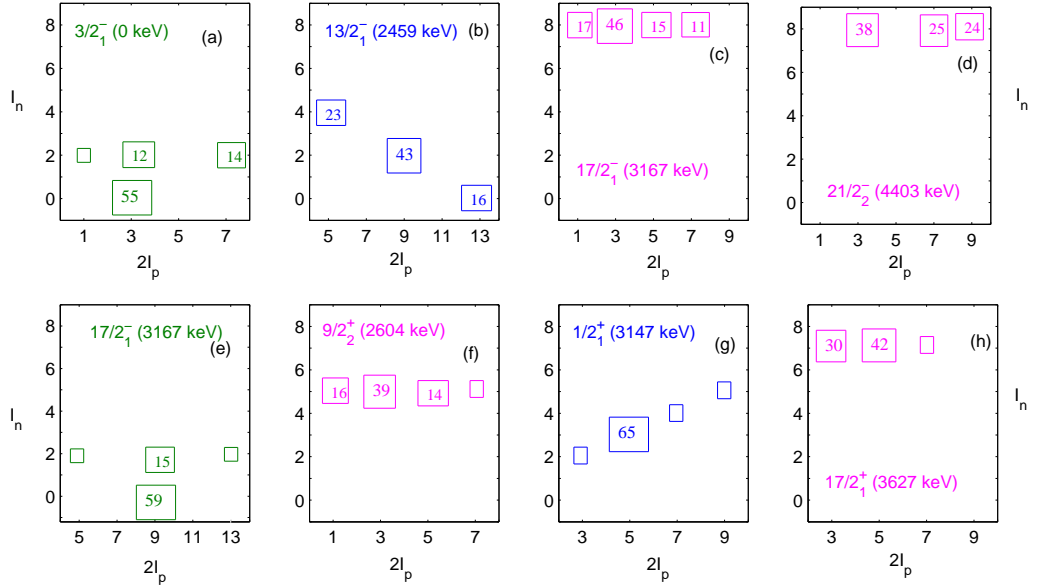


Fig. 7. Decomposition of the total angular momentum of selected states of ^{81}As into their $I_n \otimes I_p$ components. The percentage above 10% are written inside the squares, drawn with an area proportional to it. Percentage below 5% are not written.

Table 1. $B(E2)$ reduced transition strength in W.u. Effective charges $e_p = 1.5e$, $e_n = 0.5e$ / $e_p = 1.5e$, $e_n = 1.1e$ were used.

Experimental values were taken from the NNDC database.				
	^{77}As	^{79}As	^{81}As	^{83}As
BE2($5/2_1^- \rightarrow 3/2_1^-$)				
Experiment	N/A	N/A	N/A	N/A
JUN45	5.63 / 9.51	1.48 / 2.42	0.95 / 1.15	0.12 / 0.1818
jj44b	20.92 / 36.90	0.06 / 0.11	1.15 / 1.35	0.01 / 0.0212
BE2($3/2_3^- \rightarrow 3/2_1^-$)				
Experiment	> 4.4	N/A	N/A	N/A
JUN45	0.42 / 0.66	4.19 / 6.67	1.56 / 2.62	0.89 / 0.8905
jj44b	0.07 / 0.074	1.73 / 3.16	1.36 / 2.34	4.78 / 4.78
BE2($7/2_1^- \rightarrow 5/2_1^-$)				
Experiment	N/A	N/A	N/A	N/A
JUN45	2.73 / 4.31	4.10 / 6.52	0.04 / 0.0365	2.58 / 2.5839
jj44b	5.78 / 9.75	0.94 / 1.48	0.09 / 0.1162	0.17 / 0.0167
BE2($9/2_1^- \rightarrow 7/2_1^-$)				
Experiment	N/A	N/A	N/A	N/A
JUN45	1.62 / 2.52	1.72 / 2.39	0.40 / 0.4568	0.52 / 0.5231
jj44b	7.09 / 12.33	0.11 / 0.18	0.08 / 0.0668	0.58 / 0.5831
BE2($5/2_1^+ \rightarrow 9/2_1^+$)				
Experiment	80(16)	N/A	N/A	N/A
JUN45	19.39 / 29.78	17.79 / 27.426	12.10 / 18.14	5.83 / 5.83
jj44b	23.24 / 38.70	7.39 / 11.59	12.20 / 18.03	6.67 / 6.67
BE2($5/2_3^+ \rightarrow 5/2_1^+$)				
Experiment	> 0.00031	N/A	N/A	N/A
JUN45	0.004 / 0.006	0.22 / 0.36	0.21 / 0.30	0.46 / 0.46
jj44b	0.011 / 0.021	0.26 / 0.49	0.64 / 1.065	1.53 / 1.53

Table 2. $B(M1)$ values for different transitions in W.u. In the present calculation $g_s^{eff}=g_s^{free} / g_s^{eff} = 0.7 g_s^{free}$ were used.

Experimental values were taken from the NNDC database.				
	^{77}As	^{79}As	^{81}As	^{83}As
BM1($3/2_2^- \rightarrow 3/2_1^-$)				
Experiment	< 0.0041	N/A	N/A	N/A
JUN45	0.0976 / 0.4782	0.0439 / 0.0215	0.0414 / 0.0203	0.0017 / 0.00083
jj44b	0.0907 / 0.0444	0.0021 / 0.0011	0.0441 / 0.0216	0.3335 / 0.01633
BM1($3/2_3^- \rightarrow 3/2_1^-$)				
Experiment	> 0.0070	N/A	N/A	N/A
JUN45	0.0606 / 0.0297	0.0060 / 0.0029	0.0864 / 0.0423	0.0080 / 0.0079
jj44b	0.0197 / 0.0097	0.0027 / 0.0013	0.0183 / 0.0090	0.0025 / 0.0012
BM1($5/2_1^- \rightarrow 3/2_1^-$)				
Experiment	0.00193(4)	N/A	N/A	N/A
JUN45	0.0016 / 0.00078	0.0002 / 0.00011	0.0001 / 0.000055	0.0002 / 0.00011
jj44b	0.0193 / 0.0094	0.00005 / 0.0000558	0.0006 / 0.000279	0.0001 / 0.0000558
BM1($5/2_3^+ \rightarrow 5/2_2^+$)				
Experiment	> 1.9×10^{-5}	N/A	N/A	N/A
JUN45	0.0660 / 0.0312	0.0326 / 0.0159	0.000005 / 0.0000	0.0012 / 0.0006
jj44b	0.000503 / 0.0002	0.1088 / 0.0540	0.0227 / 0.0587	0.00006 / 0.00005

Table 3. Comparison of calculated and experimental magnetic and quadrupole moments. The magnetic moments, (in μ_N), with $g_s^{eff} = g_s^{free} / g_s^{eff} = 0.7g_s^{free}$ and electric quadrupole moments, Q_s (in eb), with $e_p=1.5e$, $e_n=0.5e$ / $e_p=1.5e$, $e_n=1.1e$.

	^{77}As	^{79}As	^{81}As	^{83}As
$\mu(3/2_1^-)$				
Experiment	+1.2946(13)	N/A	N/A	N/A
JUN45	+1.941 / +1.358	+2.825 / +1.977	+3.090 / +2.167	+3.666 / +2.566
jj44b	+1.477 / +1.034	+2.668 / +1.868	+2.985 / +2.089	+3.569 / +2.498
$\mu(5/2_1^-)$				
Experiment	+0.736 (22)	N/A	N/A	N/A
JUN45	+0.473 / 0.331	+0.580 / +0.406	+0.788 / +0.552	+0.915 / +0.641
jj44b	+0.406 / +0.284	+0.422 / +0.296	+0.541 / +0.379	+0.875 / +0.612
$\mu(9/2_1^+)$				
Experiment	+5.525(9)	N/A	N/A	N/A
JUN45	+5.953 / +4.167	+6.076 / +4.252	+6.335 / +4.435	+6.69 / +4.683
jj44b	+5.945 / + 4.1617	+6.032 / +4.222	+5.976 / +4.183	+6.53 / +4.571
	^{77}As	^{79}As	^{81}As	^{83}As
$Q(3/2_1^-)$				
Experiment	N/A	N/A	N/A	N/A
JUN45	+0.26 / +0.32	-0.16 / -0.21	-0.21 / -0.25	-0.12 / -0.12
jj44b	+0.27 / +0.35	-0.06 / -0.08	-0.19 / -0.23	-0.11 / -0.11
$Q(5/2_1^-)$				
Experiment	< 0.75	N/A	N/A	N/A
JUN45	-0.05 / -0.06	-0.05 / -0.07	-0.01 / -0.03	+0.13 / +0.13
jj44b	-0.09 / -0.11	-0.10 / -0.13	-0.10 / -0.14	+0.14 / +0.14
$Q(9/2_1^+)$				
Experiment	N/A	N/A	N/A	N/A
JUN45	-0.74 / -0.97	-0.68 / -0.83	-0.538 / -0.612	-0.387 / -0.386
jj44b	-0.75 / -0.97	-0.71 / -0.87	-0.536 / -0.603	-0.447 / -0.446

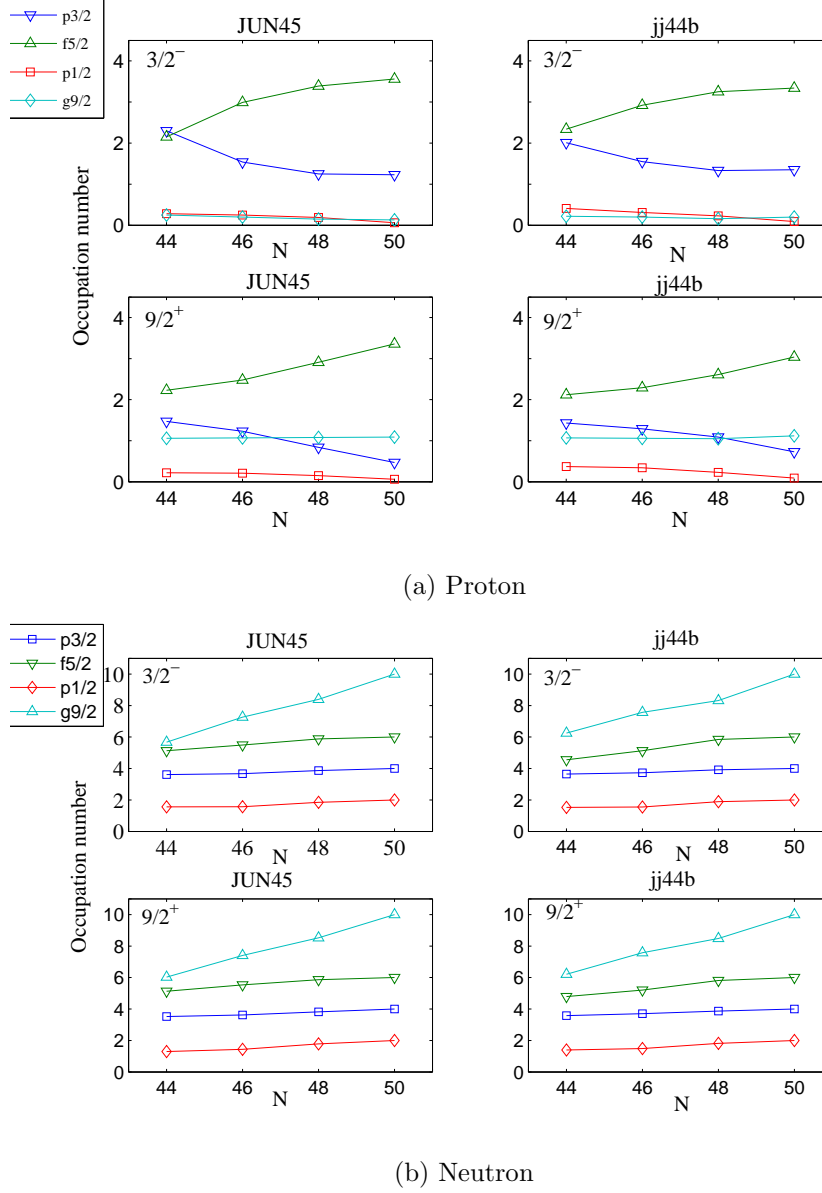


Fig. 8. (Color online) Proton/Neutron occupation numbers of the JUN45 and jj44b ($p_{3/2}$, $f_{5/2}$, $p_{1/2}$ and $g_{9/2}$ -shell orbits) interactions - for two low-lying states in $^{77,79,81,83}\text{As}$ isotopes. Upper panel for $3/2^-$; lower panel for $9/2^+$.

Acknowledgment

VK acknowledges partial financial support from CSIR, India for his PhD thesis work.

References

1. D. Steppenbeck, *et al.*, Nature **502** (2013) 207.
2. P.C. Srivastava, Mod. Phys. Lett. A **27** (2012) 1250061.
3. O. Sorlin and M. -G Porquet, Prog. Part. Nucl. Phys. **61** (2008) 602.
4. E. Sahin *et al.*, Phys. Rev. C **91** (2015) 034302.
5. K. Sieja and F. Nowacki, Phys. Rev. C **85** (2012) 051301(R).
6. S. Franchoo *et al.*, Phys. Rev. Lett. **81** (1998) 3100.
7. I. Stefanescu *et al.*, Phys. Rev. Lett. **100** (2008) 112502.
8. A. Dijon *et al.*, Phys. Rev. C **85** (2012) 031301.
9. T. Otsuka, talk at FUSTIPEN topical meeting, GANIL, Caen, France, March 17-21, 2014.
10. K. T. Flanagan, *et al.*, Phys. Rev. Lett. **103** (2009) 142501.
11. B. Cheal, *et al.*, Phys. Rev. Lett. **104** (2010) 252502.
12. M. -G Porquet, *et al.*, Phys. Rev. C **84** (2011) 054305.
13. P. Verma, *et al.*, Nucl. Phys. A **918** (2013) 1.
14. M. Honma, T. Otsuka, T. Mizusaki and M. Hjorth-Jensen, Phys. Rev. C **80** (2009) 064323.
15. B.A. Brown and A.F. Lisetskiy (unpublished).
16. E. Caurier, G. Martínez-Pinedo, F. Nowacki, A. Poves, and A. P. Zuker, Rev. Mod. Phys. **77** (2005) 427.
17. B. A. Brown, W. D. M. Rae, E. McDonald, M. Horoi, NuShellX@MSU.